FULL PAPER

Dalton
www.rsc.org/dalton

Platinum(II) diimine complexes of acetylides containing 7-azaindolyl and 2,2′-dipyridylamino functional groups †

Youngjin Kang, Junghyun Lee, Datong Song and Suning Wang *
Department of Chemistry, Queen's University, Kingston, Ontario K7L 3N6, Canada

Received 14th May 2003, Accepted 31st July 2003
First published as an Advance Article on the web 18th August 2003

Four Pt(II) diimine complexes containing acetylide ligands that are functionalized by 7-azaindolyl or 2,2′-dipyridylamino groups have been synthesized and fully characterized. Complexes **1** and **2** have the general formula Pt(bpy)-$(C{\equiv}C{-}C_6H_4\text{-}R)_2$ where bpy = 2,2′-bipyridine, R = *N*-7-azaindolyl for **1** and 2,2′-dipyridylamino for **2**, while complexes **3** and **4** have the general formula Pt(phen)$(C{\equiv}C{-}C_6H_4\text{-}R)_2$ where phen = 1, 10-phenanthroline, R = *N*-7-azaindolyl for **3** and 2,2′-dipyridylamino for **4**. The structures of **1** and **4** have been determined by single-crystal X-ray diffraction analysis. All four complexes display orange or green emission when irradiated by UV light at ambient temperature. The emission energy of **2** and **4** in solution is concentration-dependent, attributable to excimer formation at high concentrations. The utility of the 2,2′-dipyridylamino functions groups in complexes **2** and **4** was demonstrated by the interaction of **2** with Zn(II) ions *via* the dipyridyl chelating site, that leads to a change in emission intensity.

Introduction

There has been considerable interest in transition metal σ-acetylide complexes and polymers due to their various applications in non-linear optics, molecular photochemical devices, as well as supramolecular chemistry.[1] Among numerous transition metal σ-acetylide complexes, square planar platinum(II) diimine bis(acetylide) complexes, in particular, have attracted much attention recently. It has been established by Che and co-workers[2a] and many others that Pt(diimine)(arylacetylide) complexes often show bright emission in fluid solution and the solid state with a long-decay life time, arising from ^{3}MLCT. Some of the platinum(II) diimine bis(acetylide) complexes exhibit tunable orange–red emission with high quantum efficiency and long-lived MLCT excited-states,[3] making them potential emitters in electroluminescent (EL) devices and also luminescent sensors in photovoltaic cells.[4] Notably, such Pt(II) complexes have been demonstrated to have potential as chromophores in the conversion of light-to-chemical energy. For example, Eisenberg and co-workers have designed and developed dyad or triad systems, which contain either one- or two-electron donor/acceptor components in a platinum diimine chromophore.[5] These platinum diimine complexes have been shown to have long-lived excited states, attributed to metal-to-ligand charge transfer (MLCT) with contribution from Pt (dπ) and diimine (π*) orbitals.

Although there have been extensive studies on luminescence and the properties of excited states of Pt(diimine)bis(acetylide) complexes, the variation of such systems — for example, the introduction of a highly emissive and functional group into the ligand framework — remains virtually unexplored. Our recent studies have shown that 7-azaindolyl and 2,2′-dipyridylamino groups are highly emissive and capable of binding to metal ions and protons.[6] Attachment of these two functional groups to the acetylide ligands would allow us to obtain new Pt(II) diimine bis(acetylide) complexes that have vacant binding sites for potential expansion to supramolecular structures and interesting luminescent properties as well. Based on these considerations, we carried out the synthesis of several new platinum diimine bis(arylacetylide) complexes that contain blue luminescent ligands such as 7-azaindole or 2,2′-dipyridylamine with the general formula Pt(diimine)$(C{\equiv}CC_6H_4\text{-}X)_2$ with diimine = 2,2′-bipyridine, 1,10-phenanthroline, X = *N*-7-azaindole, 2,2′-dipyridylamine. Herein, we report the syntheses, crystal structures and luminescent properties of the new platinum diimine arylacetylides.

Experimental

All experiments were carried out under a dry nitrogen atmosphere using standard Schlenk techniques. Benzene, hexane and THF were freshly distilled over sodium and benzophenone. Dichloromethane was dried and distilled over P_2O_5. All starting materials were purchased from either Aldrich or Strem and used without further purification. ^{1}H, and ^{13}C NMR spectra were recorded on a Bruker Avance 300- or 400-MHz spectrometer. UV/Vis spectra were obtained on a Hewlett Packard 8562A diode array spectrophotometer with all sample concentrations in the range 10–50 μM. Excitation and emission spectra were recorded on a Photon Technologies International QuantaMaster Model 2 spectrometer. Photoluminescent lifetimes were measured on a Photon Technology International Phosphorescent lifetime spectrometer, Timemaster C-631F equipped with a xenon flash lamp, and digital emission photon multiplier tube using a band path of 5 nm for both excitation and emission. All solutions for photophysical experiments were degassed with more than three repeated freeze–pump–thaw cycles on a vacuum line. Elemental analyses were performed by Canadian Microanalytical Service Ltd., Delta, British Columbia, Canada. Melting points were determined on a Fisher-Johns melting point apparatus. Emission quantum yields of the complexes **1**–**4** were obtained relative to tris(2,2′-bipyridyl)-ruthenium(II) in degassed acetonitrile ($\Phi_r = 0.062$) at 298 K, and calculated by using previously reported procedures.[7] The absorbance of all the samples and the standard at the excitation wavelength were approximately 0.1. Cyclic voltammetry was performed using a BAS CV-50W analyzer with scan rates of 50 m V s^{-1}. The electrolytic cell used was a conventional three compartment cell, with a Pt working electrode, Pt auxiliary electrode, and Ag/AgCl reference electrode. All experiments were performed at room temperature using 0.10 M tetrabutylammonium hexafluorophosphate (TBAP)/acetonitrile as the supporting electrolyte. The ferrocenium/ferrocene couple (E_p = 0.46 V, ΔE_p = 86 mV) was used as the internal standard. Pt(bpy)Cl_2,[8] Pt(phen)Cl_2,[9] 4-(*N*-7-azaindolyl)phenylacetylene[10] and 4-(2,2′-dipyridylamino)phenylacetylene[10] were prepared by previously reported procedures.

† Electronic supplementary information (ESI) available: emission spectra of **1**–**4** in the solid state at 298 and 77 K; structures and packing diagrams of **1** and **4**. See http://www.rsc.org/suppdata/dt/b3/b305408j/

DOI: 10.1039/b305408j

Preparation of platinum diimine bis(acetylide) complexes

Complexes **1**–**4** were synthesized by using Sonogashira coupling.[11]

Method A. To a Schlenk flask containing Pt(diimine)Cl_2 and a small excess of the corresponding arylacetylene was added CuI (10 mol%), NEt_3 (5 mL) and 20 mL of degassed CH_2Cl_2. The reaction mixture was refluxed for 24 h. The initial yellow suspension became a dark red solution. After cooling, addition of water (5 mL) led to a bright orange precipitate. The solid was filtered off, washed with water and diethyl ether. Pure title complexes were isolated by using column chromatography workup on alumina (eluent: CH_2Cl_2 for **1** and **3**, CH_2Cl_2/THF (1 : 1,v/v) for **2** and **4**.)

Method B. A sample of Pt(diimine)Cl_2, CuI (10 mol%), NEt_3 (5 mL) and the corresponding arylacetylene (small excess) in CH_2Cl_2 (20–30 mL) were sonicated for 4 h. During the sonication, a bright orange precipitate was formed. The solid was filtered off, and washed with diethyl ether. Pure title complexes were also isolated by the same workup as described in method A.

Pt(bpy)(C≡CC_6H_4-*N*-7-azaindol)$_2$ (1). The procedure followed was either method A or B. However, method B gives better yields than method A. Yield: 62%; mp 148–150 °C. ^{1}H NMR in CD_2Cl_2 (δ, ppm, 25 °C): 9.86 (d, J = 5.7 Hz, 2H), 8.39 (dd, J = 4.5, 1.5 Hz, 2H), 8.22 (m, overlap, 2H, 2H), 8.02 (dd, J = 7.8, 1.8 Hz, 2H), 7.78, 7.68 (AA′BB′, J_{AB} = 8.7 Hz, 4H, 4H), 7.71 (m, overlap, 2H), 7.63 (d, J = 3 Hz, 2H), 7.18 (dd, J = 7.8, 4.5 Hz, 2H), 6.69 (d, J = 3.6 Hz, 2H). ^{13}C NMR in CD_2Cl_2 (δ, ppm, 25 °C): 157.0, 152.2, 144.1, 139.7, 133.1, 129.5, 128.4, 126.6, 123.9, 123.3, 122.2, 120.7, 118.6, 117.2, 110.7, 105.2, 102.1, 88.9. IR (KBr, pellet, cm^{-1}): ν(C≡C) 2111, 2120(sh). UV/Vis (CH_3CN): λ_{max}/nm (ε/M^{-1} cm^{-1}) 388 (7900), 306 (45 400). Anal. Calcd for $C_{40}H_{26}N_6Pt$: C, 61.41; H, 3.31; N, 10.70. Found: C, 61.39; H, 3.40; N, 10.46%.

Pt(bpy)(C≡CC_6H_4-2,2′-dipyridylamine)$_2$ (2). The procedure followed was either method A or B. However, method B also gives better yields than method A. Yield: 75%; mp 223–225 °C. ^{1}H NMR in CD_2Cl_2 (δ, ppm, 25 °C): 9.83 (d, J = 4.8 Hz, 2H), 8.30 (dd, J = 5.1, 1.2, 4H), 8.25–8.15 (m, overlap, 2H, 2H), 7.70 (dd, J = 7.2, 1.5 Hz, 2H), 7.61 (ddd, J = 15.6, 7.5, 2.1 Hz, 4H), 7.15, 7.10 (AA′BB′, J_{AB} = 8.4 Hz, 4H, 4H), 6.95–7.04 (m, overlap, 2H, 2H, 4H). ^{13}C NMR in $CDCl_3$ (δ, ppm, 25 °C): 166.2, 158.8, 148.9, 145.8, 139.6, 137.9, 133.5, 131.6, 128.8, 128.3, 127.5, 125.8, 118.7, 117.7, 102.7, 88.5. IR (KBr, pellet, cm^{-1}): ν(C≡C) 2112, 2121(sh). UV/Vis (CH_3CN): λ_{max}/nm (ε/M^{-1} cm^{-1}) 396 (5400), 308 (48 300). Anal. Calcd for $C_{46}H_{32}N_8Pt$: C, 61.94; H, 3.59; N, 12.56. Found: C, 61.52; H, 3.59; N, 12.12%.

Pt(phen)(C≡CC_6H_4-*N*-7-azaindol)$_2$ (3). The procedure followed was method B. Yield: 51%; mp 220–222 °C. ^{1}H NMR in CD_2Cl_2 (δ, ppm, 25 °C): 10.03 (dd, J = 5.1, 1.2 Hz, 2H), 8.72 (dd, J = 8.1, 1.2 Hz, 2H), 8.39 (dd, J = 4.5, 1.2 Hz, 2H), 8.08 (s, 2H), 8.01 (m, overlap, 2H, 2H), 7.80, 7.73 (AA′BB′, J_{AB} = 8.7 Hz, 4H, 4H), 7.63 (d, J = 3.6 Hz, 2H), 7.18 (dd, J = 7.8, 4.8 Hz, 2H), 6.69 (d, J = 3.6 Hz, 2H). ^{13}C NMR in CD_2Cl_2 (δ, ppm, 25 °C): 157.6, 152.7, 148.2, 144.0, 138.7, 137.1, 133.1, 131.5, 129.5, 128.3, 128.1, 126.8, 126.6, 123.9, 123.0, 122.1, 117.2, 102.1, 90.2. IR (KBr, pellet, cm^{-1}): ν(C≡C) 2113, 2123(sh). UV/Vis (CH_3CN): λ_{max}/nm (ε/M^{-1} cm^{-1}) 392 (6500), 308 (sh) (37 000), 280 (43 400). Anal. Calcd for $C_{42}H_{26}N_6Pt$ 0.5CH_2Cl_2: C, 59.89; H, 3.17; N, 9.86. Found: C, 60.13; H, 3.11; N, 9.62%. The presence of 0.5CH_2Cl_2 in the crystalline form was determined by ^{1}H NMR spectroscopy.

Pt(phen)(C≡CC_6H_4-2,2′-dipyridylamine)$_2$ (4). The procedure followed was method B. Yield: 65%; mp 238–240 °C. ^{1}H NMR in CD_2Cl_2 (δ, ppm, 25 °C): 10.0 (dd, J = 5.1, 1.2 Hz, 2H), 8.73 (dd, J = 8.4, 1.2, 2H), 8.31 (ddd, J = 4.8, 1.8, 0.6 Hz, 4H), 8.08 (s, 2H), 8.0 (dd, J = 8.1, 5.1 Hz, 2H), 7.62 (ddd, J = 15.6, 7.5, 2.1 Hz, 4H), 7.55, 7.12 (AA′BB′, J_{AB} = 8.7 Hz, 4H, 4H), 7.07 (d, J = 8.1 Hz, 4H), 6.98 (ddd, J = 7.2, 5.1, 0.9 Hz, 4H). ^{13}C NMR in $CDCl_3$ (δ, ppm, 25 °C): 165.8, 158.8, 148.9, 145.2, 137.9, 133.5, 130.5, 128.6, 128.2, 127.4, 126.0, 123.2, 118.7, 117.6, 113.5, 102.4, 89.1. IR (KBr, pellet, cm^{-1}): ν(C≡C) 2109, 2120(sh). UV/Vis (CH_3CN): λ_{max}/nm (ε/M^{-1} cm^{-1}) 392 (8800), 304 (42 900), 274 (sh) (38 900). Anal. Calcd for $C_{48}H_{32}N_8Pt$: C, 62.94; H, 3.49; N, 12.23. Found: C, 62.96; H, 3.54; N, 11.64%.

X-Ray crystallographic analysis

Single crystals of **1** were obtained from slow vapor diffusion of hexane into a solution of **1** in CH_2Cl_2/benzene. Single crystals of **4** were obtained from slow vapor diffusion of hexane/toluene into a solution of **4** in CH_2Cl_2. Data were collected on a Bruker P4 single-crystal X-ray diffractometer with a CCD-1000 detector and graphite-monochromated Mo-Kα radiation, operating at 50 kV and 30 mA at 25 °C. The data collection 2θ ranges were 4.50–56.6° for both **1** and **4**. No significant decay was observed during data collection. Data were processed on a PC using a Bruker SHELXTL software package[12] (version 5.10) and are corrected for Lorentz and polarization effects. Both compounds **1** and **4** crystallize in the triclinic space group $P\bar{1}$. All structures were solved by direct methods. Empirical absorption corrections were applied to all crystals. Solvent molecules were located in **1** (0.5 benzene and 0.5 hexane per molecule of **1**). Solvent molecules were also located in the lattice of **4** (1 CH_2Cl_2 and 0.5 hexane per molecule of **4**). The hexane molecule in **1** is disordered over two sites related by an inversion center of symmetry with a 50% occupancy for each site. It was modeled and refined successfully with each of the disordered atoms being assigned a 0.5 occupancy factor. All non-hydrogen atoms except the disordered solvent molecules were refined anisotropically. The positions of hydrogen atoms except those of the disordered solvent molecules were calculated, and their contributions to structural factor calculations were included. Crystal data for **1** and **4** are summarized in Table 1. Selected bond lengths and angles for **1** and **4** are given in Table 2.

CCDC reference numbers 210583 and 210584.

See http://www.rsc.org/suppdata/dt/b3/b305408j/ for crystallographic data in CIF or other electronic format.

Results and discussion

Syntheses and structures of the complexes

The functionalized acetylene molecules 4-(*N*-7-azaindolyl)-phenylacetylene and 4-(2,2′-dipyridylamino)phenylacetylene were synthesized using a procedure reported recently by our group.[10] The corresponding complexes Pt(diimine)(arylacetylide)$_2$, **1**–**4**, where diimine = 2,2′-bipyridine or 1,10-phenanthroline, were synthesized according to previous synthetic methodology[3a] reported by Eisenberg *et al.* by the reaction of Pt(diimine)Cl_2, diimine = 2,2′-bipyridine and 1,10-phenanthroline, with the corresponding arylacetylene in the presence of CuI/NEt_3 under either heating or sonication, as shown Scheme 1. Complexes Pt(bpy)(C≡CC_6H_4-*N*-7-azaindole)$_2$, **1** and Pt(phen)(C≡CC_6H_4-*N*-7-azaindole)$_2$, **3** were obtained in moderate yields by using both reaction conditions. However, the sonication procedure afforded a better yield for complexes Pt(bpy)(C≡CC_6H_4-2,2′-dipyridylamine)$_2$, **2** and Pt(phen)(C≡CC_6H_4-2,2′-dipyridylamine)$_2$, **4** than that obtained under heating, due to the low solubility of Pt(phen)Cl_2 in CH_2Cl_2. All complexes are soluble in common organic solvents and are stable in the solid state and in solution for several days at room temperature in the absence of light. Slow degradation of the complexes upon exposure to light was observed. Complexes **1**–**4** were fully characterized by NMR, IR and elemental

Table 1 Crystallographic data for **1** and **4**

	1	**4**
Formula	$C_{40}H_{26}N_6Pt\cdot0.5(C_6H_6)\cdot0.5(C_6H_{14})$	$C_{48}H_{32}N_8Pt\cdot(CH_2Cl_2)\cdot0.5(C_6H_{14})$
M	867.90	1043.93
Space group	$P\bar{1}$	$P\bar{1}$
a/Å	6.6498(12)	10.154(3)
b/Å	16.203(3)	13.057(3)
c/Å	17.395(4)	19.080(5)
α/°	88.544(3)	70.846(4)
β/°	83.276(4)	81.790(5)
γ/°	83.331(4)	72.416(6)
V/Å^3	1847.6(6)	2275.4(10)
Z	2	2
D_{calc}/Mg cm^{-3}	1.559	1.524
μ/mm^{-1}	3.837	3.247
No. of rflns measured	13567	13823
No. of rflns used (R_{int})	8536 (0.0527)	9491 (0.0549)
Final $R[I>2\sigma(I)]$: R_1, wR_2	0.0489, 0.0729	0.0589, 0.1171
R (all data): R_1, wR_2	0.1488, 0.1722	0.0862, 0.1437
Goodness of fit on F^2	0.695	0.850

Table 2 Selected bond lengths (Å) and angles (°) for **1** and **4**

Compound **1**			
Pt(1)–C(30)	1.934(9)	Pt(1)–C(15)	1.946(9)
Pt(1)–N(5)	2.054(7)	Pt(1)–N(6)	2.055(7)
N(1)–C(8)	1.445(10)	N(3)–C(23)	1.443(9)
C(14)–C(15)	1.183(10)	C(29)–C(30)	1.207(10)
C(30)–Pt(1)–C(15)	90.3(3)	C(30)–Pt(1)–N(5)	173.1(4)
C(15)–Pt(1)–N(5)	96.4(3)	C(30)–Pt(1)–N(6)	95.6(3)
C(15)–Pt(1)–N(6)	174.0(4)	N(5)–Pt(1)–N(6)	77.6(3)
C(1)–N(1)–C(8)	123.5(10)	C(22)–N(3)–C(23)	127.7(8)
C(35)–N(5)–Pt(1)	116.8(7)	C(31)–N(5)–Pt(1)	124.5(7)
C(14)–C(15)–Pt(1)	177.5(8)	C(29)–C(30)–Pt(1)	176.8(8)
Compound **4**			
Pt(1)–N(1)	2.059(8)	Pt(1)–N(2)	2.077(9)
Pt(1)–C(13)	1.903(12)	Pt(1)–C(31)	1.980(14)
N(4)–C(18)	1.414(13)	N(7)–C(36)	1.415(13)
C(13)–C(14)	1.222(15)	C(31)–C(32)	1.194(14)
C(13)–Pt(1)–C(31)	95.7(4)	C(13)–Pt(1)–N(1)	93.8(4)
C(31)–Pt(1)–N(1)	170.2(4)	C(13)–Pt(1)–N(2)	173.4(4)
N(1)–Pt(1)–N(2)	79.5(4)	C(12)–N(1)–Pt(1)	114.7(7)
C(14)–C(13)–Pt(1)	175.1(10)	C(32)–C(31)–Pt(1)	171.6(10)

analyses. The IR spectra for complexes **1**–**4** exhibit two bands at about 2110 and 2120 cm^{-1}, which correspond to the symmetric (ν_s) and asymmetric (ν_{as}) C≡C vibrational stretches of the acetylides in a *cis*-configuration. The crystal structures of **1** and **4** have been established by single-crystal X-ray diffraction analyses.

As shown in Fig. 1, the molecule of **1** has an approximate C_2 symmetry. The Pt atom in **1** has a somewhat distorted square

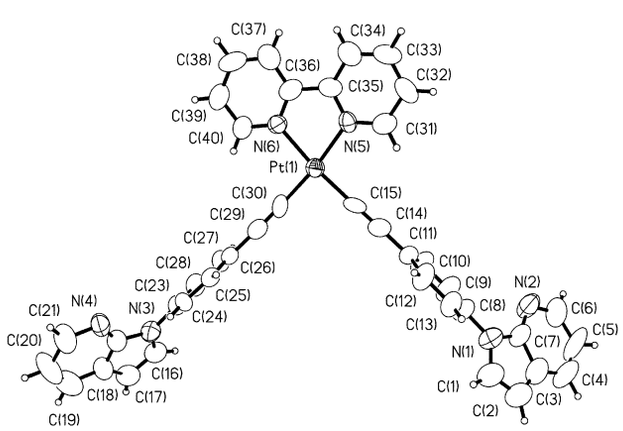

Fig. 1 A diagram showing the molecular structure of **1** with labeling schemes and 50% thermal ellipsoids.

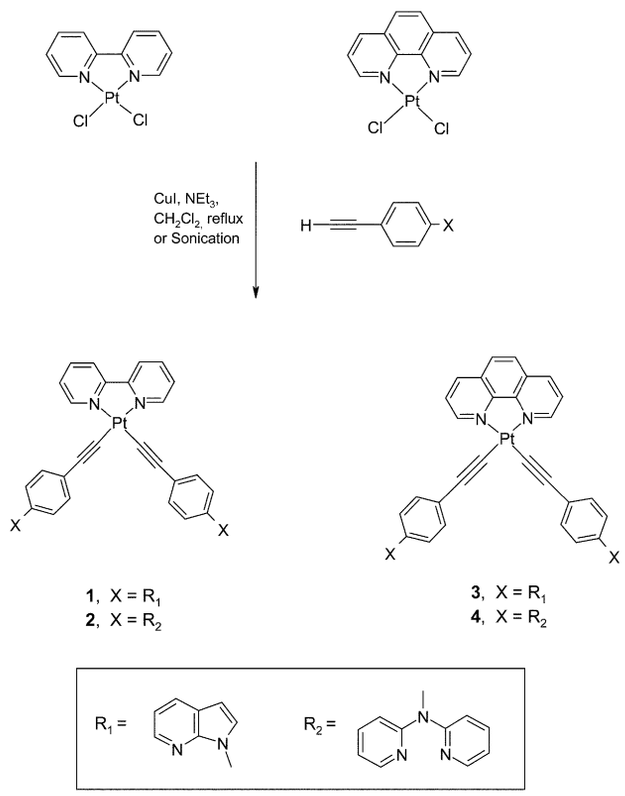

Scheme 1

planar geometry as indicated by the bond angles C(15)–Pt(1)–N(6), 174.0(4)° and C(30)–Pt(1)–N(5), 173.1(4)° (see Table 2). The Pt–N and Pt–C bond lengths are typical and similar to those of previously reported Pt(II) diimine acetylide complexes.[2,3] The acetylide ligands are coordinated to the Pt(II) center linearly as indicated by the Pt(1)–C(30)–C(29) and Pt(1)–C(15)–C(14) bond angles, 176.8(8)° and 177.5(8)°, respectively. The acetylene portion of the ligand does not appear to have significant conjugation with the phenyl ring, as indicated by the C(11)–C(14) bond length (1.438(10) Å) and C(26)–C(29) bond length (1.441(11) Å). The 7-azaindolyl group is not co-planar with the phenyl ring as indicated by the dihedral angles of 40.6° and 43.5° between the 7-azaindolyl ring and the phenyl ring of the two ligands. In the crystal lattice, molecules of **1** stack *via* the flat Pt(bpy) portion as shown in Fig. 2. The shortest intermolecular Pt–Pt separation is 4.966(2) Å. The shortest atomic separation between two neighboring bpy units is 3.32 Å, indicating the presence of significant π–π

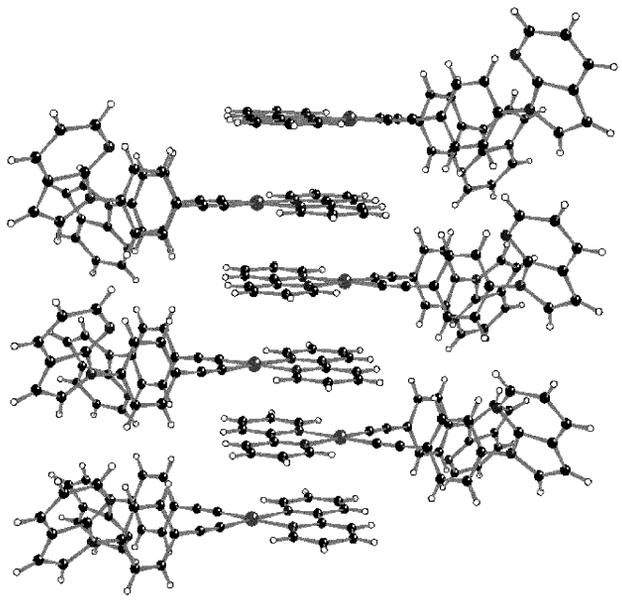

Fig. 2 A diagram showing the intermolecular π stacking of **1**.

stacking interactions. Benzene and hexane solvent molecules were located in the void channels of the crystal lattice of **1** (see ESI†). Crystals of **1** lose the lattice solvent molecules slowly upon removal from solution.

Molecules of **4** also have an approximate C_2 symmetry as shown in Fig. 3. In contrast to the structure of **1**, the Pt–acetylide portion deviates significantly from linearity, as indicated by the bond angles of Pt(1)–C(13)–C(14) and Pt(1)–C(31)–C(32), 175.1(10) and 171.6(10)°, respectively, which is clearly caused by the increased crowdedness of molecule **4** due to the presence of the 2,2′-dipyridylamino unit. The amino nitrogen atom lone pair electrons do not appear to conjugate with the phenyl ring, as indicated by the dihedral angles between the C(17) phenyl ring and the C(26)–N(4)–C(21) plane (121.2°) and the C(38) phenyl ring and the C(43)–N(7)–C(44) plane (54.7°). The dihedral angles between the phenyl ring and the pyridyl rings range from 57.7–102.3°. The molecules of **4** stack in pairs through the flat Pt(phen) portion in the crystal lattice as shown in Fig. 4 with the intermolecular Pt–Pt separation between the pair being 4.767(2) Å. The shortest atomic separation between the two neighboring phenanthroline ligands is 3.44 Å, again indicating the presence of significant π–π stacking interactions. CH_2Cl_2 and hexane solvent molecules are located in the crystal lattice of **4**. Crystals of **4** slowly lose the lattice solvent molecules at ambient temperature.

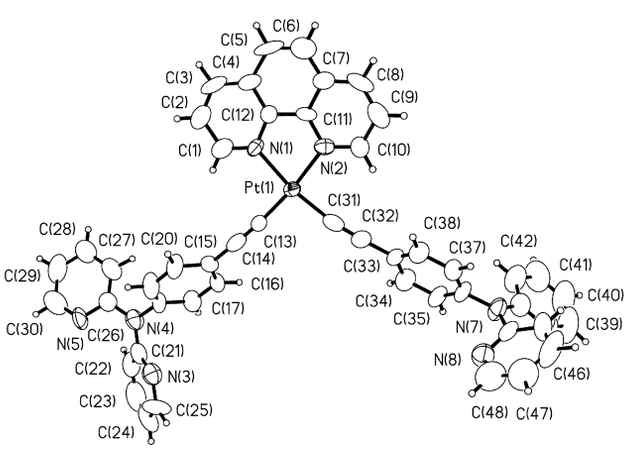

Fig. 3 A diagram showing the molecular structure of **4** with labeling schemes and 50% thermal ellipsoids.

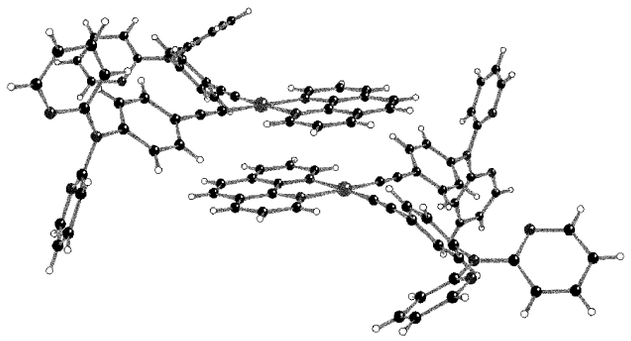

Fig. 4 A diagram showing the π stacked dimer of **4**.

Electrochemical properties

Complexes **1**–**4** display a reversible reduction wave at E_p $(1/2(E_p^a + E_p^c)) = -0.80$ V ($\Delta E_p = 0.87$ mV), −0.706 (ΔE_p = 0.87 mV), −0.76 V ($\Delta E_p = 0.60$ mV), and −0.78 V ($\Delta E_p = 0.81$ mV), respectively (*versus* Ag/AgCl), which can be attributed to a one-electron reduction of the diimine ligand.[2,3,13] For compounds **3** and **4** a second reduction wave at $E_p = -1.09$ V (ΔE_p = 0.51 mV) and −1.03 V ($\Delta E_p = 0.50$ mV), respectively, was also observed, which may be caused by the further reduction of the coordinated phenanthroline ligand.[13] Compound **4** displayed an irreversible oxidation wave at 1.23 V, which is likely due to the one-electron oxidation of the Pt(II) ion to a Pt(III) ion. The electrochemical properties of complexes **1**–**4** are consistent with those of previously known Pt(II) diimine complexes.[2,3,13]

Luminescence properties

The free ligands *p*-HC≡CC_6H_4-*N*-7-azaindole and *p*-HC≡CC_6H_4-2,2′-dipyridylamine have fluorescence emissions in the 370–400 nm region when irradiated by UV light. The 2,2′-bipyridine and 1,10-phenanthroline ligands also display an emission peak at $\lambda_{max} \approx 380$ nm in solution. These emissions are attributed to π–π* transitions. In contrast, the Pt(II) acetylide complexes **1**–**4** display quite different luminescence properties (see Table 3).

As shown in Fig. 5, the UV/Vis spectra of **1**–**4** all display a weak and broad MLCT band in the region of 350–500 nm, characterized by a characteristic solvachromic shift, in addition to the intense π–π* transition absorption bands of the ligands. The absorption maximum of the MLCT band for compounds **1**–**4** in benzene, CH_2Cl_2, THF, acetone, methanol, DMF and CH_3CN is summarized in Table 4. The solvent column in Table 4 is arranged in the order of increasing dipole moment (*e.g.* benzene has a zero dipole moment while DMF has the highest dipole moment (3.86) among the solvents listed). In general, the MLCT band for the four complexes appears to shift toward a shorter wavelength with an increase in the dipole moment of the solvent with the exception of the DMF solutions.

The emission spectra of **1**–**4** in CH_2Cl_2 solution at 298 K and in a CH_2Cl_2 glass 77 K are shown in Fig. 6. For complexes **1** and **3** orange phosphorescent emission was observed in solution at ambient temperature and green emission was observed in the solid state at ambient temperature. Interestingly, upon the removal of the solvent molecules from the crystal lattice of **1** under reduced pressure, the emission color of **1** changed from green to orange. At 77 K, the emission band of **1** and **3** is blue shifted to the green region, which is likely caused by the increased rigidity of the solution medium at 77 K and the slowing down of solvent interactions with the complex. A blue shift of the emission band with a decrease in temperature has also been observed in some other luminescent complexes and is described as "luminescence rigidochromism".[14a–c] An excellent account on solvent and temperature effects on luminescence can be found in Lakowicz's book.[14d] Based on the results of a previous study on 2,2-bipyridine and 1,10-phenanthroline

Table 3 Photoluminescence data for **1**–**4**[a]

Compound	Absorption[b] MLCT (λ_{max}/nm)	Emission (λ_{max}/nm)	Quantum[c] yield (Φ_{em})	Life time/μs	Conditions
1	402 (7900)	589	0.067	4.9	Solution, 298 K
		533		239	Solution, 77 K
		542		8.3	Solid, 298 K
		546		183	Solid, 77 K
2	406 (5400)	571	0.016	1.3	Solution, 298 K
		523		234	Solution, 77 K
		565		4.2	Solid, 298 K
		565		221	Solid, 77 K
3	398 (6500)	576	0.045	3.9	Solution, 298 K
		542		189	Solution, 77 K
		548		5.8	Solid, 298 K
		542		164	Solid, 77 K
4	398 (8800)	590	0.005	6.1	Solution, 298 K
		538		210	Solution, 77 K
		573		6.0	Solid, 298 K
		567		212	Solid, 77 K

[a] Concentration: [M] = 4.5×10^{-5} M^{-1}. [b] In CH_2Cl_2 solution at 298 K. [c] The quantum yields of all compounds were obtained by comparing to tris(2,2′-bipyridyl)ruthenium(II).

Table 4 Absorption and emission for MLCT of **1**–**4** in various solvents

	1		**2**		**3**		**4**	
Solvent	λ_{abs}/nm	λ_{em}/nm	λ_{abs}/nm	λ_{em}[a]/nm	λ_{abs}/nm	λ_{em}/nm	λ_{abs}/nm	λ_{em}[a]/nm
Benzene	424	588	424	520	418	582	424	526
THF	416	593	416	544	410	590	410	563
CH_2Cl_2	402	589	406	523	398	576	398	538
Acetone	402	586	404	530	398	587	398	550
CH_3OH	388	565	384	532	388	545	384	536
CH_3CN	388	581	396	540	392	581	392	546
DMF	398	572	402	537	398	582	397	536

[a] At 77K.

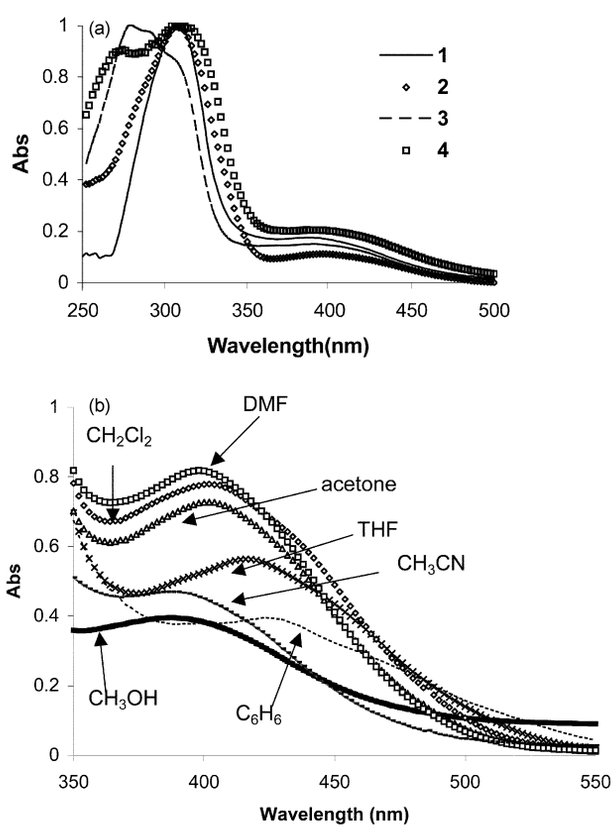

Fig. 5 Top: UV/Vis absorption spectra of complexes **1**–**4** in acetonitrile at 298 K. Bottom: UV/Vis spectra showing the MLCT band of **1** in various solvents at 298 K.

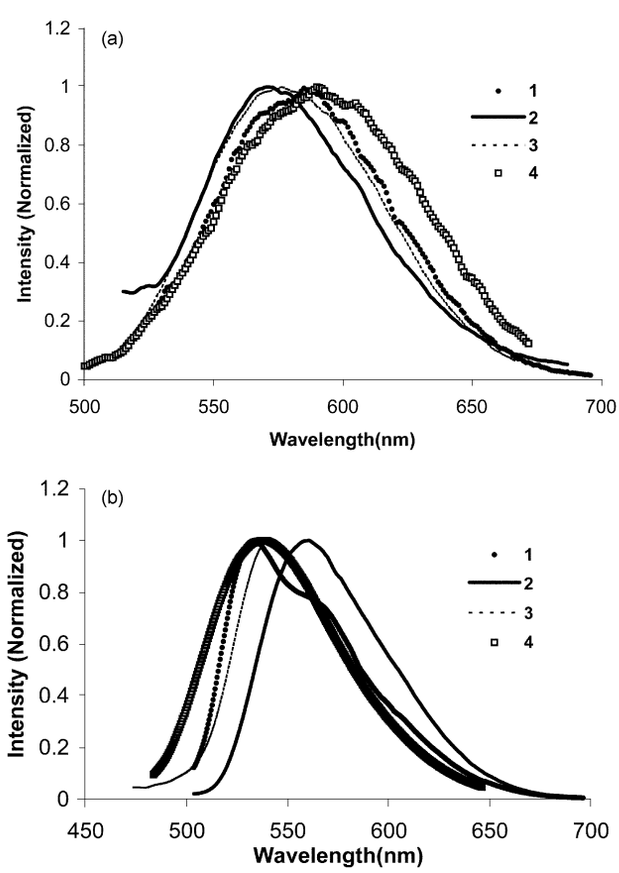

Fig. 6 Top: emission spectra of **1**–**4** in CH_2Cl_2 at 298 K. Bottom: emission spectra of **1**–**4** in CH_2Cl_2 at 77 K.

complexes of Pt(II) containing acetylide ligands,[2,3] we believe that the phosphorescent emission of **1** and **3** likely originates from MCLT transitions. Complexes **2** and **4** also display green emission in the solid state at ambient temperature. An emission color change from green to orange was also observed for the solid of **4**, when the solvent molecules were driven out of the crystal lattice under reduced pressure. An intriguing phenomenon is that in solution, the emission energy of **2** and **4** at ambient temperature is concentration-dependent (Fig. 7). At very low concentration ($<10^{-5}$ M), the emission band is in the blue-violet region, resembling that of the free *p*-HC≡CC_6H_4-2,2′-dipyridylamine ligand, the bpy ligand and the phen ligand. As the concentration increases, the emission intensity decreases and the emission energy shifts toward longer wavelength. For example, at $\approx 10^{-4}$ M, the emission of **2** is dominated by a very weak phosphorescent emission band with λ_{max} at 570 nm. A similar phenomenon was also observed for **4**. The concentration-dependent behavior of **2** and **4** is reminiscent of that of [Pt(4,7-diphenyl-1,10-phenthroline)$(CN)_2$] investigated by Volger *et al.*,[15] who attributed the emission band at low concentration to [Pt(4,7-diphenyl-1,10-phenthroline)$(CN)_2$] to ligand centered π–π* transitions and the emission band at relatively high concentrations to an excimer emission involving either intermolecular π–π interactions or direct Pt–Pt interactions. In the intermediate concentration range, Volger *et al.* suggested that metal-centered, ligand-centered and MLCT transitions are all likely to contribute to the lowest energy absorption and emission bands. Based on our crystal structure data, it seems that the excimer emissions for **2** and **4** are likely caused by interligand (bipy or phen) π–π interactions. At 77 K, the emission bands of **2** and **4** in a frozen solution resemble those of **1** and **3** and do not change with concentration. The 77 K emission bands of **1**–**4** in frozen CH_2Cl_2 solutions can be obtained using the MLCT excitation energy (≈400 nm). Therefore, we believe that they originate from MLCT transitions. The long emission lifetimes (190–240 μs) of compounds **1**–**4** in CH_2Cl_2 at 77 K (Table 3) are consistent with those of previously reported MLCT emissions of Pt(diimine)X_2 complexes.[2,3,13]

One important feature of molecules **1**–**4** that distinguishes them from the previously known Pt(diimine)X_2 compounds is the presence of a 7-azaindolyl or a 2,2′-dipyridylamino functional group. These functional groups bear lone pair electrons, and hence can coordinate or interact with a metal ion. Such interactions may lead to a change of luminescence. To confirm this, we examined the interaction of $ZnCl_2$ with complex **2** in solution by monitoring the emission spectrum of **2** either in a low concentration solution (1.0×10^{-5} M) at ambient temperature or in a frozen solution (1.0×10^{-5} M, CH_2Cl_2, 77 K). As shown in Fig. 7, the phosphorescent emission peak (at 77 K) was gradually quenched with an increase in $ZnCl_2$ content. In contrast, however, the ligand-centered fluorescent emission of **2** at ambient temperature gained intensity substantially, as the $ZnCl_2$ content was increased. In addition, the shape of the fluorescent emission band also changes with an increase in $ZnCl_2$. The interaction of the $ZnCl_2$ unit with complex **2** clearly has an opposite effect on the low energy emission (dominating at 77 K, or at a high concentration at ambient temperature) and

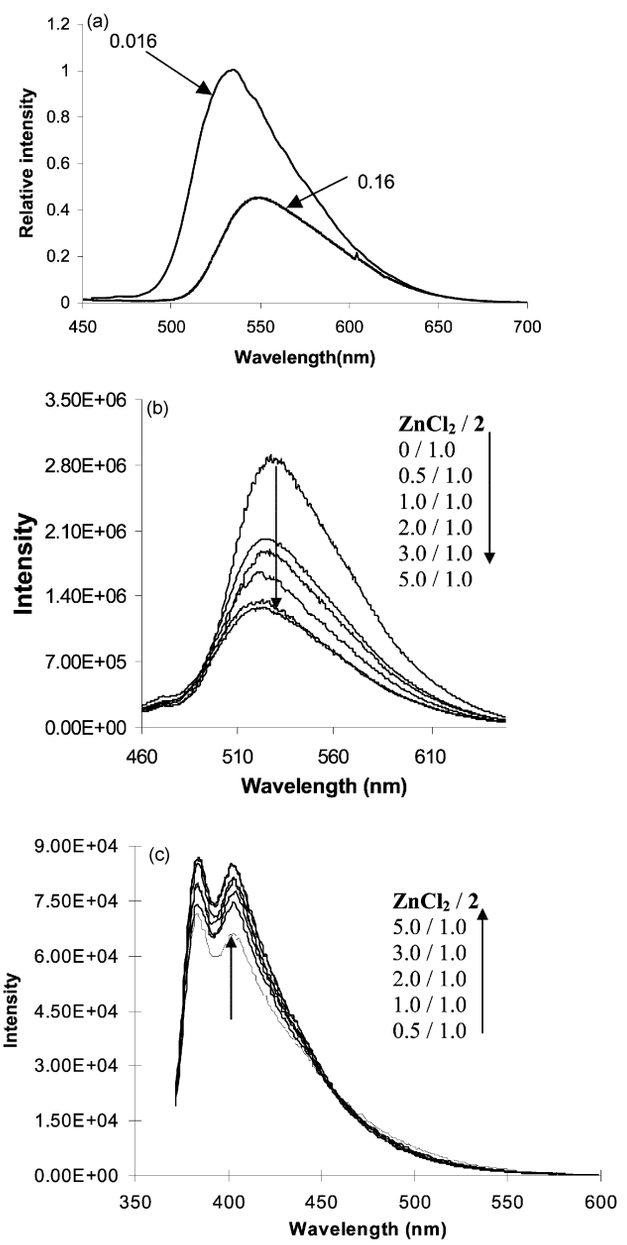

Fig. 7 Top: emission spectra of complex **2** at 0.16 mM and 0.016 mM. Middle: emission spectral change of **2** in frozen CH_2Cl_2 at 77 K (1.0×10^{-5} M) in the presence of $ZnCl_2$. Bottom: emission spectral change of **2** at 298 K in CH_2Cl_2 (1.0×10^{-5} M) in the presence of $ZnCl_2$.

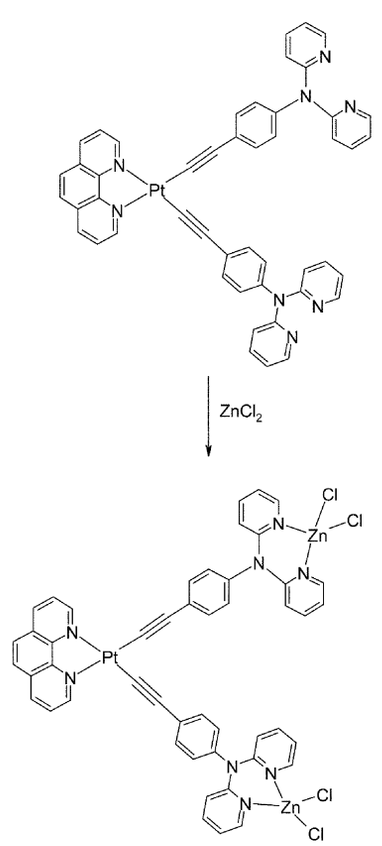

Scheme 2

the high energy emission band (dominating at a low concentration at ambient temperature). The details are yet to be understood. Nonetheless, we believe that the chelating interaction as depicted in Scheme 2 must be responsible for the emission quenching/enhancing phenomenon and that such coordination interaction may be useful for the potential applications of complexes **1**–**4** as luminescent sensors for metal ions. Further investigation on the interactions of **1**–**4** with various metal ions is currently being conducted.

Conclusions

In summary, four novel Pt(II) diimine complexes containing 2,2′-dipyridylamino and 7-azaindolyl functionalized arylacetylide ligands have been synthesized and fully characterized. These complexes display MLCT charge transfer and orange–green phosphorescence in solution and in the solid state. They are potentially useful as luminescent sensors/probes for metal ions.

Acknowledgements

We thank the Natural Sciences and Engineering Research Council of Canada for financial support.

References

1 (*a*) J. Manna, K. D. John and M. D. Hopkins, *Adv. Organomet. Chem.*, 1995, **38**, 79; (*b*) I. Manners, *Angew. Chem., Int. Ed. Engl.*, 1996, **35**, 1602; (*c*) R. P. Kingborough and T. M. Swager, *Prog. Inorg. Chem.*, 1999, **48**, 123; (*d*) N. J. Long, C. Langhoff and M. E. Thompson, *J. Am. Chem. Soc.*, 1992, **114**, 7560; (*e*) N. Hagihara, K. Sonogashira and S. Takahashi, *Adv. Polym. Sci.*, 1981, **41**, 151; (*f*) J. Manna, C. J. Kuehl, J. A. Whiteford, P. J. Stang, D. C. Muddiman, S. A. Hofstadler and R. D. Smith, *J. Am. Chem. Soc.*, 1997, **119**, 11611; (*g*) K. Onitsuka, M. Fujimoto, N. Ohshiro and S. Takahashi, *Angew. Chem., Int. Ed.*, 1999, **38**, 689; (*h*) P. Nguyen, P. Gómez-Elipe and I. Manners, *Chem. Rev.*, 1999, **99**, 1515.

2 (*a*) C. W. Chan, L. K. Cheng and C. M. Che, *Coord. Chem. Rev.*, 1994, **132**, 87–97; (*b*) S. D. Cummings and R. Eisenberg, *J. Am. Chem. Soc.*, 1996, **118**, 1949.

3 (*a*) M. Hissler, W. B. Connick, D. K. Geiger, J. E. McGarrah, D. Lipa, R. J. Lachicotte and R. Eisenberg, *Inorg. Chem.*, 2000, **39**, 447; (*b*) E. C. Whittle, J. A. Weinstein, M. W. George and K. S. Schanze, *Inorg. Chem.*, 2001, **40**, 4053; (*c*) W. B. Connick, D. Geiger and D. R. Eisenberg, *Inorg. Chem.*, 1999, **38**, 3264; (*d*) Y. Ng, C. M. Che and S. M. Peng, *New J. Chem.*, 1996, **20**, 781.

4 (*a*) M. Hissler, J. E. McGarrah, W. B. Connick, D. K. Geiger, S. D. Cummings and R. Eisenberg, *Coord. Chem. Rev.*, 2000, **208**, 115; (*b*) S. C. Chan, M. C. W. Chan, Y. Wang, C. M. Che, K. K. Cheung and N. Zhu, *Chem. Eur. J.*, 2001, **7**, 4180.

5 J. E. McGarrah, Y. J. Kim, M. Hissler and R. Eisenberg, *Inorg. Chem.*, 2001, **40**, 4510.

6 (*a*) Y. Kang, C. Seward, D. Song and S. Wang, *Inorg. Chem.*, 2003, **42**, 2789; (*b*) Y. Kang, D. Song, H. Schmider and S. Wang, *Organometallics*, 2002, **21**, 2413; (*c*) S. Wang, *Coord. Chem. Rev.*, 2001, **215**, 79; (*d*) Q. Liu, L. Thorne, I. Kozin, D. Song, C. Seward, M. D'Iorio, Y. Tao and S. Wang, *J. Chem. Soc., Dalton Trans.*, 2002, **16**, 3234; (*e*) S. F. Liu, Q. Wu, H. L. Schmider, H. Aziz, N. X. Hu, Z. Popovic and S. Wang, *J. Am. Chem. Soc.*, 2000, **122**, 3671; (*f*) J. Ashenhurst, G. Wu and S. Wang, *J. Am. Chem. Soc.*, 2000, **122**, 2541; (*g*) Q. Wu, M. Esteghamatian, N. X. Hu, Z. Popovic, G. Enright, S. R. Breeze and S. Wang, *Angew. Chem., Int. Ed.*, 1999, **38**, 985; (*h*) J. Pang, Y. Tao, X. P. Yang, M. D'Iorio and S. Wang, *J. Mater. Chem.*, 2002, **12**, 206; (*i*) Q. Wu, Q. A. Hook and S. Wang, *Angew. Chem., Int. Ed.*, 2000, **39**, 3933; (*j*) D. Song, Q. Wu, A. Hook, I. Kozin and S. Wang, *Organometallics*, 2001, **20**, 4683; (*k*) Q. Wu, J. A. Lavigne, Y. Tao, M. D'Iorio and S. Wang, *Chem. Mater.*, 2001, **13**, 71.

7 (*a*) S. J. Strickler and R. A. Berg, *J. Chem. Phys.*, 1962, **37**, 814; (*b*) E. M. Kober, J. L. Marshall, W. J. Dressick, B. P. Sullivan, J. V. Caspar and T. J. Meyer, *Inorg. Chem.*, 1985, **24**, 2755.

8 G. R. Newkome, K. J. Theriot, F. R. Fronczek and B. Villar, *Organometallics*, 1989, **8**, 2513.

9 K. D. Hodges and J. V. Rund, *Inorg. Chem.*, 1975, **14**, 525.

10 Y. Kang and S. Wang, *Tetrahedron Lett.*, 2002, **43**, 3711.

11 Y. Fujikura, K. Sonogashira and N. Hagihara, *Chem. Lett.*, 1975, 1067.

12 SHELXTL NT Crystal Structure Analysis Package, Version 5.10, Bruker AXS, Analytical X-ray Systems, Madison, WI, 1999.

13 D. Collison, F. E. Mabbs, E. J. L. McInnes, K. J. Taylor, A. J. Welch and L. J. Yellowlees, *J. Chem. Soc., Dalton Trans.*, 1996, 329.

14 (*a*) S. Wang, G. Garzon, C. King, J. C. Wang and J. P. Fackler, Jr., *Inorg. Chem.*, 1989, **28**, 4623; (*b*) A. J. Lees, *Chem. Rev.*, 1987, **87**, 711; (*c*) G. J. Ferraudi, *Elements of Inorganic Photochemistry*, John Wiley & Sons, New York, 1988; (*d*) J. R. Lakowicz, *Principles of Fluorescence Spectroscopy*, 2nd edn., Kluwer Academic/Plenum, New York, 1999, ch. 6.

15 (*a*) H. Kunkely and A. Vogler, *J. Am. Chem. Soc.*, 1990, **112**, 5625; (*b*) C. N. Pettijohn, E. B. Jochnowitz, B. Chuong, J. K. Nagle and A. Vogler, *Coord. Chem. Rev.*, 1998, **171**, 85.